A Hybrid Model and MIMO Control for Intelligent Buildings Temperature Regulation over WSN

**Emmanuel WITRANT, Stéphane MOCANU,
Olivier SENAME**

*Control Systems Department, UJF/INPG, Université de Grenoble
(e-mail: [Emmanuel.Witrant, Stephane.Mocanu, Olivier.Sename]
@gipsa-lab.inpg.fr).*

Abstract: The aim of this paper is to propose a model-based feedback control strategy for indoor temperature regulation in buildings equipped with underfloor air distribution (UFAD). Supposing distributed sensing and actuation capabilities, a $0-D$ model of the ventilation process is first derived, based on the thermodynamics properties of the flow. A state-space description of the process is then inferred, including discrete events modeled by Markovian processes. This results in a hybrid model with nonlinear components. The use of a wireless sensor network (WSN) and the resulting communication constraints are also discussed. A H_∞ MIMO controller is finally proposed and shown to effectively handle the discrete and nonlinear perturbations.

1. INTRODUCTION

Intelligent buildings ventilation control is a challenging automation problem with objectives that rise several research problems of immediate actuality, such as the wireless automation and the control of complex interconnected subsystems. The system considered is composed of ventilated rooms, fans, plenums and a wireless network. The complexity arises from the different physical properties - and associated dynamics - of the subsystems. In a broader picture, all these engineering problems imply to deal with fluid models and the connection of different subsystems. Global control strategies are of prime importance to deal with such problems.

Recent results have illustrated the interest for under floor air distribution (UFAD) solutions in comparison with traditional ceiling-based ventilation (Center for the Built Environment (CBE) (2002)). An UFAD indoor climate regulation process is set with the injection of a fresh airflow from the floor and an exhaust located at the ceiling level, as depicted in Fig. 1. Note that we consider the specific case where a common plenum is used at both the underfloor and ceiling levels. It has been established that well-designed UFAD systems can reduce life-cycle building costs, improve thermal comfort, ventilation efficiency and indoor air quality, conserve energy, and reduce floor-to-floor height. Feedback regulation, as considered in this paper, is a key element for an optimized system operation and it can be achieved thanks to actuated diffusers and distributed measurements provided by a wireless sensor network (WSN) deployed in the ventilated area.

Global regulation strategies are particularly difficult to establish for such plants, due to the system complexity and the real time constraints. In order to set a model-based
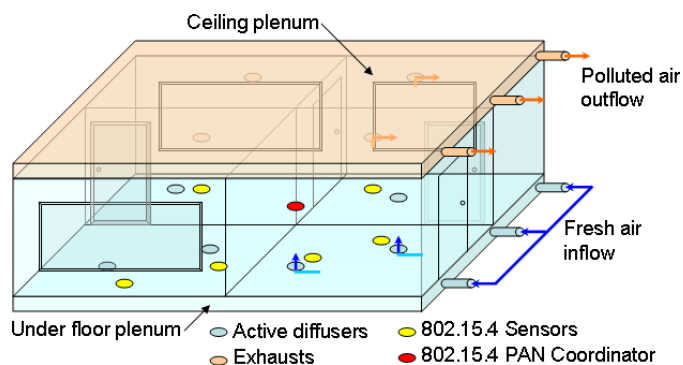

Fig. 1. UFAD ventilation

control approach, we first investigate the thermodynamics properties of the ventilation process with a *control volume* approach. We will show that it allows for a reduced-order, easily reconfigurable system description but implies nonlinearities and discrete events (doors, internal power sources, etc.). Such events are handled specifically with an Markovian approach and the resulting system is described as a hybrid state-space model. The distributed sensing capabilities associated with the WSN are considered by proposing a specific network architecture and highlighting the related communication constraints (bandwidth limitation and time delays).

The purpose of this paper is to describe the main dynamics associated with UFAD feedback regulation and illustrate the use of the resulting model in a simple control strategy. In this sense, it is not aimed here to design a controller which will vary according to the stochastic processes (i.e. a multi-mode controller) but actually to ensure that the control strategy will be robust enough to cope with variations
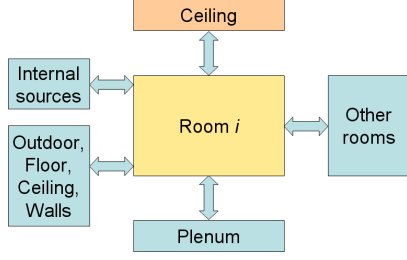
Fig. 2. Bloc representation

and disturbances due to Markovian processes. The H_∞ control approach has then be selected due to its intrinsic robustness property, a systematic design procedure, and its efficiency in a wide range of applications, in particular with time-delays as illustrated in Sename and Fattouh (2007).

The paper is organized as follows. First, the UFAD process is described as an interconnected model in Section 2. This model is used in Section 3 to obtain a hybrid state-space description, including the Markovian processes. Section 4 details the deployment of the WSN. The design of a H_∞ controller is described in Section 5. Finally, the model behavior and the controller efficiency are illustrated thanks to simulation results in Section 6.

2. UFAD MODEL

In order to provide a model that is suited for real-time feedback control, we consider a 0-D model based on the mass and energy conservation in each room. Each room is interconnected with the other building elements as depicted in Fig. 2. The interconnections are fully defined, for the choice of any couple of components, by the mass flow rate and heat transport. A generic and flexible model of an UFAD system is thus obtained thanks to an appropriate classification of the mass and heat sources, combined with the continuity equation and the first and second laws of thermodynamics in each room. In comparison with more thorough models such as $EnergyPlus^{\text{TM}}$ (US department of energy (2008)), our approach is focused on the flexibility of its application and on the key dynamics for control purposes.

2.1 Continuity and conservation of energy

The room dynamics is set using fundamental laws of thermodynamics, described in classical textbooks such as Sonntag et al. (1998). The internal state of room i, described by its density and temperature $< \rho_i, T_i >$, is determined based on the following hypotheses:

H1. the flow is incompressible: $\rho_i = \rho_{air}$;
H2. the control volume (CV) remains constant relative to the coordinate frame;
H3. the state of mass within the CV is uniform at any time;
H4. the state of the mass crossing the CV is constant with time (the mass flow rates may vary);
H5. the kinetic and potential energy of the gas within the room are neglected.

The first assumption is straightforward considering the low speed of the airflow within the rooms. (H2)-(H4)

are classical for *uniform-state, uniform-flow* processes, i.e. when there is no change in the state of mass (we consider only gas in our case). (H5) is associated with the fact that the gas moves slowly in the room and that the mass of the gas in the CV is not important enough to generate significant potential energy. The CV considered is strictly limited to the inside room volume: it does not include the underfloor and ceiling plenums.

The continuity equation, along with incompressibility (H1), implies that the mass conservation writes as:

$$\sum \dot{m}_{in_i} = \sum \dot{m}_{out_i}, \qquad (1)$$

where $\dot{m}_{in}$ and $\dot{m}_{out}$ are the input and output mass flow rates, respectively. The first law of thermodynamics, applied with (H2)-(H4) and without mechanical work, gives the energy exchange in the room CV as:

$$\frac{dE_i}{dt} = \dot{Q}_i + \sum \dot{m}_{in_i} h_{tot,in_i} - \sum \dot{m}_{out_i} h_{tot,out_i},$$

where E_i is the room energy, $\dot{Q}_i$ the heat exchange and h_{tot} the total enthalpy, approximated as $h_{tot} = C_p T$ with C_p the constant pressure specific heat. Considering (H5), the room energy is the internal energy (constant volume) and $E_i = \rho_{air} V_i C_v T_i$, where V_i is the room volume and C_v is the constant volume specific heat. For air at $25°C$ and 1 atm, $C_v = 717$ $J/kg.K$, $C_p = 1004$ $J/kg.K$ and $\rho_{air} = 1.169$ kg/m^3.

The heat exchange Q_i can be decomposed, depending on the nature of the heat transfers, as:

- conduction (Fourier's law): $\dot{Q}_{cond} = kA\Delta T/\Delta x$, where k $[W/m.K]$ is the conductivity (≈ 10 for glass, 0.1 for insulation materials) and A the surface area where exchanges occur;
- convection (Newton's law): $\dot{Q}_{conv} = Ah\Delta T$, where h $[W/m^2]$ is the heat transfer coefficient (typically within the range $5 - 25$ for natural convection and 25-250 for forced convection, sometimes expressed in $[W/m^2.K]$);
- radiation (electromagnetic waves): $\dot{Q}_{rad} = \epsilon\sigma AT_s^4$, where ϵ is the emissivity (0.92 for nonmetalic surfaces), $\sigma = 5.67 \times 10^{-8}$ $Wm^{-2}K^{-4}$ is the Stephan-Boltzmann constant and T_s is the surface temperature.

Under the previous hypotheses, the mass flow rate $\dot{m}$ going from a high temperature volume T_h to a low temperature volume T_l through a section A is obtained by combining Bernoulli's and the ideal gas equations as:

$$\dot{m} = \rho A\sqrt{2R(T_h - T_l)} \qquad (2)$$

where $R = C_p - C_v$.

2.2 Room dynamics

Based on the previous description, we obtain the room temperature dynamics:

$$\frac{dT_i}{dt} = \frac{1}{\rho_{air} V_i C_v} \left[\dot{Q}_{conv} + \dot{Q}_{cond} + \dot{Q}_{rad} + \dot{Q}_{sources} \right.$$
$$\left. + C_p \sum \dot{m}_{in_i} T_{in_i} - C_p \sum \dot{m}_{out_i} T_i \right],$$

Component	Associated energy
Inside walls iw	$-k_{iw}A_{iw}(T_i - T_j)/\Delta x_{iw}$
Outside walls ow	$-\left(k_{ow}\frac{A_{ow}}{\Delta x_{ow}} + k_{glass}\frac{A_{glass}}{\Delta x_{glass}}\right)(T_i - T_{out})$
Plenum pl	$C_p\dot{m}_{pl}T_{pl}$
Floor	$-k_{pl}A_{pl}(T_i - T_{pl})/\Delta x_{pl}$
Ceiling c	$-C_p\dot{m}_cT_i$
People b	$\epsilon\sigma A_b(T_b^4 - T_i^4)$
Inside sources	$\dot{Q}_{sources}$
Doors d	$C_p\rho A_d\sqrt{2R(T_j - T_i)}T_j$, if $T_j > T_i$
	$C_p\rho A_d\sqrt{2R(T_i - T_j)}T_i$, if $T_i > T_j$

Table 1. Energy sources in room i.

where we introduced the additional source $\dot{Q}_{sources}$ to model the internal heat sources (computers, printers, etc.) and considered the outflow temperature as the room temperature (which is a direct consequence of the 0-D approximation). A simplified classification of the heat sources for room i is proposed in Table 1, where T_j indicates the temperature in an adjacent room, A_x the exchange surface areas and Δx_x the thicknesses. Note that the last three components correspond to discrete events while the previous ones have continuous variations. This description is easily refined by introducing additional terms (walls radiation, windows airflow, etc.), depending on the desired level of model accuracy.

The continuity constraint implies that:

$$\dot{m}_{c_i} = \sum_{l=1...N_{pl}} \dot{m}_{pl_i,l} + \sum_{l=1...N_d} \dot{m}_{d_{ij},l}.$$

where N_{pl} is the number of diffusers in the room and N_d denotes the number of doors. The doors mass flow rate can be computed thanks to (2) as $\dot{m}_d = sign(T_j - T_i)\rho A_d\sqrt{2R|T_j - T_i|}$, where the $sign$ function is introduced to indicate the flow direction. The temperature regulation is achieved by controlling the mass flow rate from the plenum $\dot{m}_{pl_i,l}(t)$ and the underfloor temperature $T_{pl}(t)$. We will suppose in the following that there is only one diffuser per room ($N_{pl} = 1$) and that the WSN provides the temperature measurements for the feedback law.

Finer models, including the height-dependency of the temperature variations, can be derived using the stratified flow theory Yih (1969) or buoyancy driven flow dynamics Gladstone and Woods (2001). The WSN measurements can also be set to determine the temperatures distribution shape, along the lines suggested in Sandou et al. (2008). Future works may include a convective model of the flow as a time-delay, constrained by the conservation laws described above.

3. HYBRID STATE-SPACE MODEL

3.1 Continuous dynamics

The continuous dynamics of the model is set by the walls, ceiling and plenum. According to the physical laws described in Section 2.2 and supposing all the doors to be closed, we have that:

$$\frac{dT_i}{dt} = \frac{1}{\rho_{air}V_iC_v}[-(\Xi_i + C_p\dot{m}_{pl_i})T_i + \sum_{l=1...N_{iw}} \alpha_{iw_l}T_l$$
$$+ \sum_{l=1...N_{ow}} (\alpha_{ow_l} + \alpha_{glass_l})T_{out}$$
$$+ (C_p\dot{m}_{pl_i} + \alpha_{pl_i})T_{pl_i}], \qquad (3)$$
$$\Xi_i \doteq \sum_{l=1...N_{iw}} \alpha_{iw_l} + \sum_{l=1...N_{ow}} (\alpha_{ow_l} + \alpha_{glass_l}) + \alpha_{pl_i},$$

where $\alpha_x = k_xA_x/\Delta x_x$ for component x, N_{iw} is the number of connected inside walls and N_{ow} is the number of outside walls.

Defining the state as the vector containing the rooms temperatures $x = [T_1 \; T_2 \; ...T_n]^T$, the controlled inputs as $u \doteq [\dot{m}_{pl_i} \; T_{pl}]^T$ and the exogenous input as $w \doteq T_{out}$, the system dynamics write as:

$$\frac{dx}{dt} = (A_1 + A_2(u))x + (B_1 + B_2(u))u + B_ww$$
$$\doteq f_c(x, u, w),$$

where the state matrices $A_{1,2}$ and the input matrices $B_{1,2,w}$ are computed according to (3). The function f_c is introduced to denote the continuous part of the model in a compact form. Note that this model is fully determined by the building architecture and constant physical variables.

3.2 Discrete events

The complete dynamics of the system is described by the following differential equations systems with stochastic jumps :

$$\frac{dx}{dt} = f_c(x, u, w) + P\mathcal{P}(x - Ux) + s + \mathcal{H}(Y, x), \qquad (4)$$

where U is a permutation matrix, s is a vector providing informations on the exogenous heat sources, $\mathcal{P}$ is an operator over temperature differences between adjacent rooms implementing the formula in the "Doors" line of Table 1 and P is a matrix providing the status of the communication doors (open/close). The humans drifting between rooms is modeled by the random walk process Y while $\mathcal{H}$ is a functional on Y and x corresponding to the formula in Table 1. The impact of the discrete event part of the model on the system dynamics is described among the entries of P, s, Y and $\mathcal{H}$.

For the numerical part within the scope of this paper we neglect the contribution of human sources as the people drifting between rooms needs several supplementary assumptions whose confirmation needs a lot of statistical data. The heat produced by human bodies is then simply considered as a power source combined with the computers operation.

The vector $(x - Ux)$ provides the information on the relative temperature difference between rooms. The permutation matrix U is chosen such that Ux is a shift of x. Let:

$$U = \begin{bmatrix} 0 & 1 & 0 & 0 \\ 0 & 0 & 1 & 0 \\ 0 & 0 & 0 & 1 \\ 1 & 0 & 0 & 0 \end{bmatrix}. \qquad (5)$$
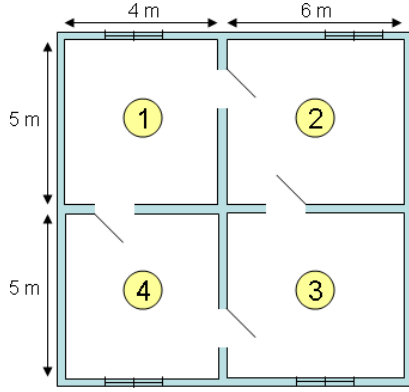
Fig. 3. Flat architecture for the test case

3.3 Discrete Event model of exogenous heat sources

We consider as exogenous heat source any device in a room (a computer for example) which heats the room during its ON periods. We consider that such a heat source has a constant contribution during ON periods and zero contribution during OFF periods (we ignore the cooling time after switching OFF the device). Then the entries of the vector s are the outputs of Markovian independent processes. The states of each Markovian process corresponds to the total power of the ON devices. In the simplest case (all the heat sources in a room are identical) the Markovian process is a finite birth and death process.

3.4 Discrete Event model of heat transfer through open doors

The contribution of a door heat transfer to the dynamics dx_j/dt of the temperature of room j is expressed as $p_i\mathcal{P}(x_{j_1} - x_j)$ where $p_i = 0$ if the door i is closed and $p_i = 1$ if door i is open, and x_{j_1} is the temperature of the room accessible through door i. We consider the example presented in Fig. 3: each room has two doors (two neighboring rooms) and the doors are labeled from 1 to 4 such that door i relates rooms i and $i + 1$ for $i = 1..3$. Door 4 relates rooms 4 and 1. Let p_i be a 0 or 1 valued variable expressing the status of a door. Then the entries of the matrix P are equal to $\pm p_i$ or 0 if there is no door between rooms. The matrix P is then:

$$P = \begin{bmatrix} p_1 & 0 & 0 & p_4 \\ p_1 & p_2 & 0 & 0 \\ 0 & p_2 & p_3 & 0 \\ 0 & 0 & p_3 & p_4 \end{bmatrix}. \tag{6}$$

The variables p_i are obtained as the output of Markovian processes describing the circulation between the rooms. For the instance we will assume independence of the random processes. Further research will study the influence of correlation between processes (independence means that people are circulating only between neighboring rooms, correlation corresponds to longer travels - for example passing from room 1 to 3 needs openings of doors 1 and 2).

4. WIRELESS SENSOR NETWORK

Our sensor network is set in a star topology around a Personal Area Network (PAN) coordinator. The best real-
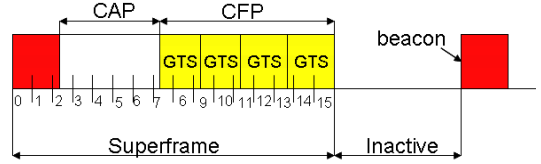

Fig. 4. Superframe structure in beacon-enabled mode

time performance in 802.15.4 is achieved in a coordinated network using 2.4GHz frequency band and Offset Quadrature Phase-Shift Keying (O-QPSK, see Zheng and Lee (2006)) modulation.

4.1 IEEE 802.15.4 real-time support

In Zheng and Lee (2006) an exhaustive study of the real-time performance of IEEE 802.15.4 was presented. Our conclusions are based mostly on this study. Two medium access methods are available in coordinated low-rate wireless PAN (LR-WPAN) : beacon-enable mode and non-beacon-enable mode. Non-beacon-enabled mode uses a non deterministic medium access method and therefore is not suitable for real-time applications. In beacon-enabled mode a Contention Free Period (CFP) is defined which implements a fairly good deterministic support for real-time applications.

4.2 Beacon-enabled mode

In beacon-enable mode the WPAN behavior is driven by synchronisation signals (beacons) sent by the PAN coordinator. The beacon interval defines the transmission period of the network. According to 802.15.4 standard the beacon interval is divided between an active period (called superframe) and a power saving period (inactive). The superframe is divided in 16 slots which are allocated to the beacon frame, the Contention Access Period (CAP) and the Contention Free Period. The CAP period uses a random access transmission and has no real-time interest. The CFP period is divided in reserved slots (called Guaranteed Time Slots - GTS) which are allocated to devices by the PAN coordinator. The overall structure of the superframe and the beacon interval is presented in Fig. 4. The existence of GTS provides the real-time support of 802.15.4 networks.

Unfortunately there are two limitations in the 802.15.4 superframe which decreases the real-time performance. Firstly a minimal length of the CAP period has to be preserved. Secondly, the maximal number of allocatable GTS is limited to 7.

4.3 Communication constraints

The real-time performance of the beacon-enabled LR-WPAN networks depends on several parameters which control the superframe structure and length. We examine the choice of the various parameters from the point of view of the control system.

The performance measures of interest here are : the end-to-end propagation delay and the maximal polling rate. While we assume only CFP transmission there are no back off frames. It follows that the only source of delay

is the pure radio waves propagation delay which, given the low distances (around 15m) and the high radio waves propagation speed, it is of order of ns and can be neglected.

We turn out to the study of the maximal polling rate (equivalently, the minimal sampling period). While a communication cycle is defined by the beacons, a high polling rate is achieved by short beacon intervals. However, there is a trade-off between the superframe duration and the number of polled sensors in a superframe. The optimization of the maximal polling rate is dependent on the number of sensors managed by the PAN coordinator.

The following variables are controlling the superframe :

System variables (cannot be modified):

- Minimal CAP Length : 440 bytes;
- Base Slot Duration : 60 bytes;
- Beacon maximal size : 127 bytes;
- interframe : 12 for short frames (< 18 symbols);
- MAC frame overhead : 13 for 2 bytes MAC adresses;
- Physical frame overhead : 6 bytes.

Application variables:

- Superframe duration (controlled by the superframe order - SO and the base slot duration BSD)

$$SD = \#slots \times BSD \times 2^{SO} = 960 \times 2^{SO}$$

  The legal values of SO can range between 0 and 14.

One can see from the above formula for the superframe duration that a 802.15.4 frame is between 15.36 ms (for SO=0 at 62.5Kbytes/s) and 251.6 s (for SO=14 also at 256 kbps).

Then, the minimal sampling period that can be used is 15.36 ms. However, SO=0 frames assume an important protocol overhead (more than 50% of the frame is used by the beacon and CAP). Then a very important step in communication tuning is to verify that the available capacity of the superframe can acquire the necessary communication data.

In our setup we assume that the LR-WPAN is used only for data acquisition from the sensors. Then, our system will require only 4 GTS for retrieving data from the 4 sensors. Assume that the sensors use accurate 24-bits A/DC. Then, each GTS needs between 26 and 46 bytes (3 payload, 11 to 31 overhead, 12 interframe). In a superframe of order 0, only 5 or 6 base slots are available (8 are used by CAP, and 2 are used by the beacon). In order to insure that our sensors can pe polled in a single order 0 superframe we have simply to chose short (2 bytes) MAC addressing, which induces 31 bytes overhead and then requires a single base slot GTS. The time delay can be assumed to twice the superframe duration due to the local processing time (i.e. 30.72 ms).

5. ROBUST MIMO H_∞ CONTROL

5.1 Some background on H_∞ control

This part states the problem in a way similar to Skogestad and Postlethwaite (1996) where more details can be found. H_∞ control is formulated using the general control configuration (I) in Fig. 5 where $\mathcal{P}(s)$ is the generalized plant

model, w is the exogenous input vector, v is the control input vector, e is the controlled output vector and y is the measurement vector.

Given γ, a pre-specified attenuation level, an H_∞ suboptimal control problem is to design a controller that internally stabilizes the closed-loop system and ensures:

$$\|N_{ew}(s)\|_\infty \leq \gamma \qquad (7)$$

where $N_{ew}(s)$ is the closed-loop transfer matrix from w to e. The minimal value γ_{opt} is then obtained as:

$$\gamma_{opt} = \min_K \| N_{ew}(s) \|_\infty \qquad (8)$$

In general, some weights are considered on the controlled outputs (including the actuator force). They represent the performance specifications in the frequency-domain. $\mathcal{P}$ thus includes the plant model G and the considered input and output weights (W_i, W_o) as depicted in Fig. 5 (II).
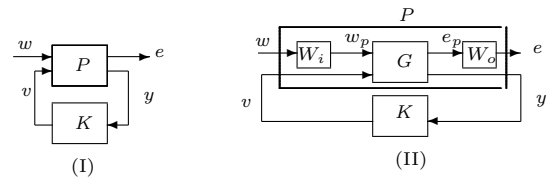

Fig. 5. General control configuration

The H_∞ control problem is then referred to as a mixed sensitivity problem, W_i and W_o thus appearing in (7) as weights on the sensitivity functions. The usual way of solving the H_∞ control problem is the use of Riccati equations or LMI. Note that the LMI solution consists in applying the Bounded Real Lemma to the closed-loop system (where the state matrices of the controller are unknown). The resulting optimization problem is a Bilinear one, which is solved using the projection lemma as explained in Scherer et al. (1997). The result relies on two LMI and the reconstruction of the controller matrices follows using an equivalent system transformation.

5.2 The H_∞ building control design

The controller consists in a MIMO temperature regulation of $x = [T_1 \ T_2 \ \ldots T_n]^T$, using the control inputs $u \doteq [\dot{m}_{pl_1} \ \dot{m}_{pl_2} \ \ldots \dot{m}_{pl_n} \ T_{pl}]^T$. However (4) is a nonlinear model. To cope with the linear H_∞ control design the model has been simplified by considering the dominant modes only (corresponding to A_1) and assuming a constant temperature for the plenum (linearized input matrix $\bar{B}$). Thus the control model is simply given by:

$$\dot{x} = A_1 x + \bar{B}u + B_w w.$$

According to Fig. 5, v is the control input to be designed, $y = [T_1 \ T_2 \ \ldots T_n]^T$ is the vector of measured outputs, and $w = r$ represents the external inputs (here the 4 temperature references). The global controlled outputs are $e = (e_z^T, e_u^T)^T$, where $e_u = W_u v$ is the weighted control input and $e_z = W_z(r-y)$ the weighted controlled output (the output weight on Fig. 5 (II) is then $W_o = diag(W_u, W_z)$). The input weight W_i stands for the disturbance weight, chosen to be constant here ($w_p = w_d w$).

Note that the matrix W_z of weighting functions is chosen as:

$$W_z = diag(W_{z1}, W_{z2}, \ldots, W_{zn}).$$

The weighting functions (W_z, W_u) have been chosen according to the industrial performance specifications.
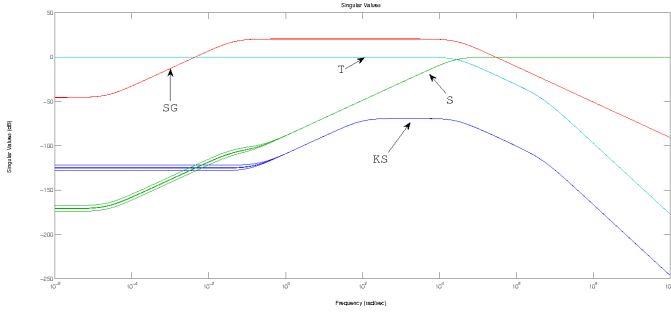

Fig. 6. Singular values plot of the sensitivity functions, S, T, KS and SG

6. SIMULATION RESULTS

We consider the specific building architecture presented in Fig. 3, with 2 m^2 windows in each room and walls conductivity properties inferred from Corgnati et al. (2008) (averaged values).

The simulation results are given in Fig.7 for the following scenario. The room temperatures are initially: $T_1 = T_4 = 301\ K$ and $T_2 = T_3 = 299\ K$. Each room temperature is set to a desired value with $T_1^{ref} = T_4^{ref} = 297\ K$ and $T_2^{ref} = T_3^{ref} = 293\ K$, at the successive instants (for each room) $t = 500, 750, 1000, 1250\ s$, respectively. It can then be seen that the room temperature control strategy is efficient, even if we experience noticeable variations, due to the stochastic processes and nonlinear effects.

7. CONCLUSION

In this work, we considered the problem of temperature regulation in intelligent buildings as the real-time control of an actuated UFAD process based on WSN measurements. A flexible model of the airflows was proposed based on the thermodynamics properties of the room control volume. Discrete events such as doors openings, people presence and the use of computers or printers were introduced as Markovian 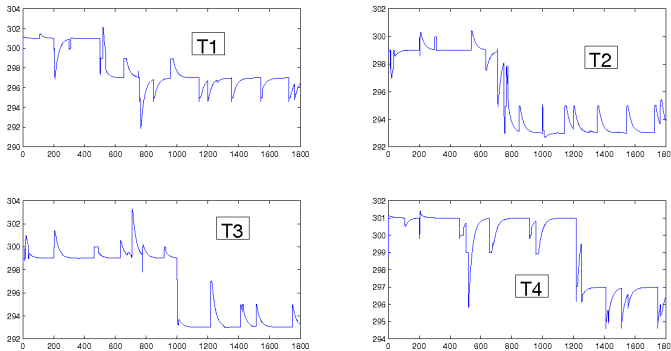processes, which resulted in a hybrid nonlinear state-space description of the complete interconnected system. The deployment of the WSN was detailed and shown to introduce communication constraints such as bit-rate limitations and time-delays. A MIMO H_∞ controller regulating the linearized model dynamics and tuned to reject the unpredictable discrete perturbations was finally designed and shown to effectively achieve the feedback objectives on simulation results.

REFERENCES

Center for the Built Environment (CBE) (2002). Design guide on underfloor air distribution systems. Technical report, ASHRAE.

Corgnati, S., Fabrizio, E., and Filippi, M. (2008). The impact of indoor thermal conditions, system controls and building types on the building energy demand. *Energy and Buildings*, 40, 627–636.

Gladstone, C. and Woods, A. (2001). On buoyancy-driven natural ventilation of a room with a heated floor. *J. Fluid Mech.*, 441(293–314).

Sandou, G., Witrant, E., Olaru, S., and Niculescu, S. (2008). Receding horizon climate control in metal mine extraction rooms. In *Proc. of the IEEE Conference on Automation Science and Engineering*. Washington DC, USA.

Scherer, C., Gahinet, P., and Chilali, M. (1997). Multiobjective output-feedback control via LMI optimization. *IEEE Trans. Autom. Control*, 42(7), 896–911.

Sename, O. and Fattouh, A. (2007). Robust h_∞ control of bilateral teleoperation systems under communication time-delay. In J. Loiseau and J. Chiasson (eds.), *Applications of Time Delay Systems*, LNCIS. Springer.

Skogestad, S. and Postlethwaite, I. (1996). *Multivariable Feedback Control: analysis and design*. John Wiley and Sons.

Sonntag, R., Borgnakke, C., and Van Wylen, G. (1998). *Fundamentals of Thermodynamics*. John Wiley & Sons, 5th edition.

US department of energy (2008). *EnergyPlus^{TM} Engineering Reference*.

Yih, C.S. (1969). Stratified flows. *Annu. Rev. Fluid Mech.*, 1, 73–110.

Zheng, J. and Lee, M.J. (2006). *Sensor Network Operations*, chapter 4.3 Comprehensive Performance Study of IEEE 802.15.4., 218–237. Wiley – IEEE Press.

Fig. 7. Room temperatures evolution